HiSST: 3rd International Conference on
High-Speed Vehicle Science Technology
14 -19 April 2024, Busan, Korea

SWBLI EFFECTS OF IMPINGING SHOCK ON A FLAT PLATE IN HIGH MACH NUMBER FLOW

Aishwarya PS[1], Mohammed Ibrahim Sugarno[1]

Abstract

The present work examines the shock-wave boundary layer interaction resulting from the impingement of an oblique shock wave, created by a 38° wedge, on a flat plate in a flow with a Mach number 6. The primary emphasis of the analysis is centered on the attainment of Mach reflection, wherein the Mach stem serves as a distinctive attribute for observing the Edney Type II shock interaction occurring on the flat plate. This research is aimed to examine the two-dimensional implications of variation of height of the wedge from the flat plate or vertical distance ratio (h/w) to observe its influence on the Mach stem height and various other flow properties contributing to the change. The phenomena of separation and the length of separation bubble are also studied due to the influence of h/w ratio. Computational fluid dynamic analysis using the Ansys Fluent solver is employed for the study.

Keywords: *SWBL, Mach stem, Mach Reflection, Edney Type II interference.*

Nomenclature

P_∞ - Freestream Pressure

T_∞ - Freestream Temperature

M_∞ - Freestream Mach number

h_∞ - Freestream Enthalpy

Re_∞/l -Unit Reynolds number

β_{LS} – Leading edge shock angle

β_{SS} – Separation shock angle

h/w - Vertical distance ratio

T_0 – Total Temperature

1. Introduction

Shock wave boundary layer interaction (SWBLI) is a phenomenon of complex and dynamic interplay between the adverse pressure gradient due to shock wave and the boundary layer due to no-slip conditions on surfaces. This interaction is noticed in many cases such as – an oblique shock impingement on a flat surface, ramp-induced SWBL interaction, normal or near normal shock boundary interactions in air intakes and shock tubes, and interactions in presence of obstacle in forward or backward facing step as shown in Fig. 1. Within the framework of SWBLI, the shock wave itself can be considered as a passive phenomenon for the boundary layer, acting solely as a source of an adverse pressure gradient. The primary concern lies in the response of the boundary layer to this imposed pressure gradient, particularly the phenomenon of separation prevalently known as strongly interacting flows. The boundary layer separation, however, is not an isolated event. It triggers the generation of shock patterns within the adjacent inviscid flow, ultimately impacting the entire flow field. In this situation, the

[1] *Hypersonic Experimental Aerodynamics Laboratory (HEAL), Department of Aerospace Engineering, Indian Institute of Technology, Kanpur 208016, India, ibrahim@iitk.ac.in*

interaction is said to be a purely strong viscous – inviscid interaction [5] where viscous effects must be contemplated while fully anticipating the flow field.

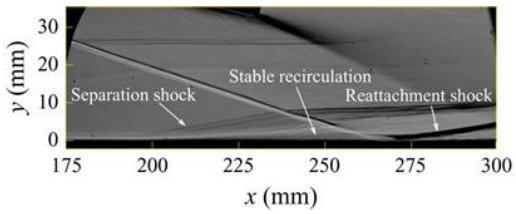

(a) Oblique shock impingement on flat plate [1]

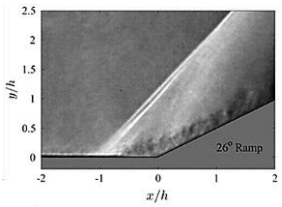

(b) Ramp-induced SWBLI [2]

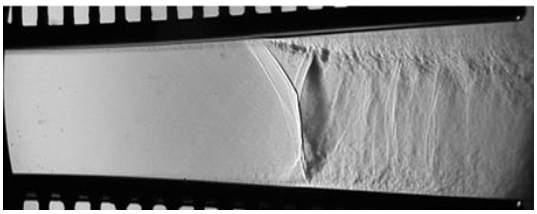

(c) SWBLI in nozzle flow. [3]

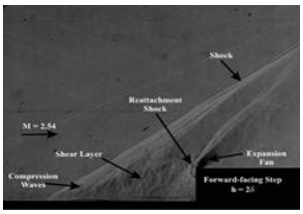

(d) SWBLI in FFS.[4]

Fig 1. Examples of cases where interaction between shock wave & boundary layer is observed.

The reflections of plane shock from a plane surface can be deduced into regular reflection (RR) and Mach reflection (MR) [6] where the transition occurs from RR to MR [7] with a near normal shock or Mach stem as a distinguished feature in MR. The shock pattern that occurs in Mach reflection because of boundary layer separation can be classified as Edney Type II interaction [9] with Mach stem forming between two triple points as shown in Fig. 2. This complex interaction between a strong impinging oblique shock (C_1) and separation shock (C_2) from separated boundary layer formulates into the creation of near normal shock (m) between to triple points TP_1 and TP_2 in Fig. 2(b). The subsonic medium behind this Mach stem is accelerated by continuous supersonic flow until a sonic throat arises. The stagnation pressure loss due to this near normal shock is adverse in the case of high-speed air intake [10].

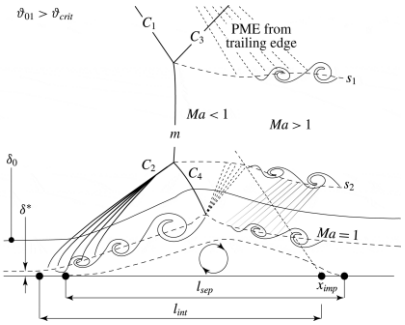

(a) Schematic illustration of MR.

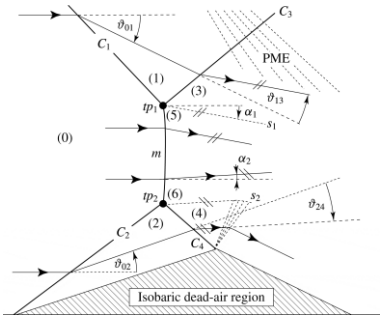

(b) Inviscid flow model for MR**.**

Fig 2. Edney Type II interaction in viscous flow condition arising Mach reflection [8].

Over the past 75 years, the effects of SWBLI in the case of impinging shock have been extensively researched in analytical, numerical, and experimental methods. The experimental observations for the upstream influence and transitional studies for laminar and turbulent boundary layers for freestream Mach number 1.3 to 1.5 have been obtained [11]. Experimental studies have been carried out at Mach number 2.15 for impinging oblique shock on the laminar boundary layer, which showed good agreement numerically for the positions of separation and reattachment and downstream velocity profiles [12]. Recently, quantitative studies at hypersonic flight conditions have been carried out to observe the onset of separation in the laminar boundary layer with wall pressure and heat transfer measurements to analyze transitional behaviour for impinging shock in RR case [1].

Extensive research has been conducted in supersonic and hypersonic flow regimes, particularly focusing on transitional flow behaviour, the upstream and downstream influence on the boundary layer, separation and reattachment points, and variation of separation length with shock strength, while the influence of Mach number and Reynolds number have been reported independently for laminar and turbulent boundary layer [14][15]. However, this research has primarily been limited to RR. Studies have reported that the Mach reflection due to an oblique impinging shock can be observed with sufficiently high Mach number flows or higher shock strength [5]. An experimental investigation of impinging shock-boundary layer interaction observed a near normal shock for a 6 mm blunt leading edge at M = 5.88, allowing the determination of the reflected shock strength [16]. Through analytical methods studied in compressible open jets one can analyze the Mach stem height and estimate the extent of the subsonic region which allows prediction of transition from RR to MR. As stated, in open jets the Mach stem configurations are unique for given conditions, while the Mach stem shock structure in wedge flows is dependent on geometry of wedge, i.e. w/H value [17]. There have been numerous reports on transitional studies from RR to MR clearly stating that transition occurs at von Neumann condition and not at detachment condition in a steady flow [18] and variation of cowl turning angle [13], and hysteresis phenomenon studies during transition have been studied at von Neumann angle [20].

In addition, there have been several numerical investigations of MR in inviscid flows and they have been reported comprehensively for the case of double wedge configurations observing sensitivity of RR to MR for various schemes [20], numerical studies on wedge boundary layer correction methods to observe the effects of Mach stem height [21] and large eddy simulations to analyze the classical two and three-shock theory to derive the stability criteria for MR [22] have been reported in extensive.

Nevertheless, limited research studies have been conducted on MR in high Mach number and at higher wedge angle much nearer to the flow detachment angle. Hence, a parametric study between the oblique shock impingement and boundary layer phenomenon (by varying crosswise/vertical) is carried out to study the behaviour of Mach stem height and separation bubble.

2. Geometric model and description

The proposed model for SWBL interaction to obtain MR for an impinging oblique shock is composed of wedge with an angle of 38° and length of compression face, w to be 55mm, where the oblique shock resulting from the wedge is directed towards the flat plate of length (l) 200 mm as shown in Fig. 3. The wedge angle is determined based on the θ-β-M relation for the specified free-stream conditions in Table 1, aiming to achieve a high shock strength by selecting a wedge angle close to the maximum flow deflection angle (θ_{max}) for the given Mach number, thereby facilitating the desired Mach reflection (MR).The strength of an oblique shock can be varied by changing the h/w in crosswise/vertical direction.

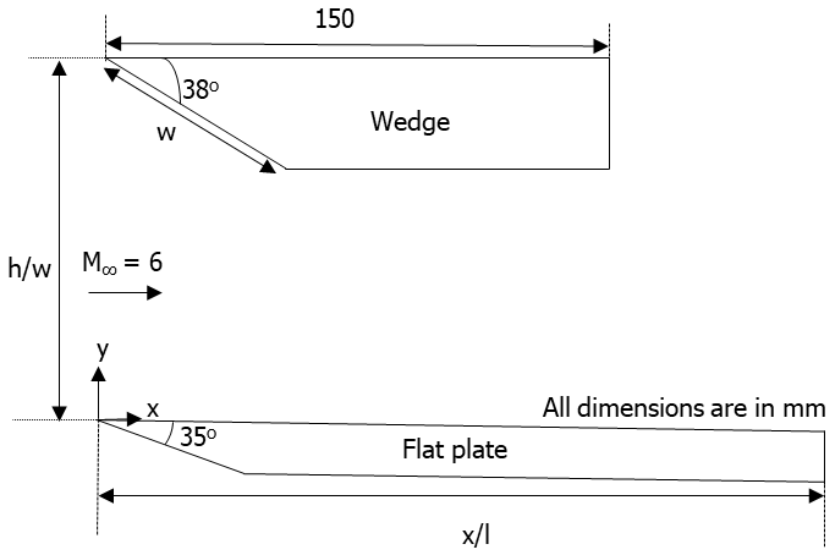

Fig 3. Schematic illustration of the model for impinging shock case to obtain Mach reflection.

3. Numerical methods

3.1. Governing equation

A numerical simulation of the above flow field is conducted using the commercial software ANSYS Fluent, which leverages the finite volume method. The simulation is governed by the two-dimensional, compressible, unsteady Reynolds-averaged Navier-Stokes (RANS) equations with detached eddy simulation (DES) model for SST $k-\omega$ turbulence model considering Sutherland's law for viscosity. The DES model is referred as hybrid LES/RANS combined where the unsteady RANS model is employed in boundary layer, while the LES is applied to separated regions where the large unsteady turbulence plays a major role [23]. Two-dimensional inviscid simulations are carried out by solving Euler equations [24] to understand the shock impingement location and the corner expansion effect on the oblique shock. The working fluid is assumed to be ideal gas and freestream conditions are listed in Table 1.

Table 1: Free stream properties

P_∞	M_∞	T_∞	T_o	Re_∞/l
480 Pa	6	36.5 K	300 K	15.63 x 10^6 m^{-1}

3.2. Computational grid and boundary condition

The structured computational grid of the model is generated using commercial software ANSYS Mesh Workbench. The dimension of the domain is varied according to change in h/w. The computational domain and boundary conditions for $h/w = 1.82$ are shown in the Fig. 4. The pressure far-field boundary conditions are applied to top and lateral surfaces of the domain for the free stream conditions. The pressure outlet boundary condition is applied to the downstream of the domain, while the pressure inlet boundary condition is applied to the upstream of the domain. The no-slip adiabatic wall boundary conditions are applied to the wall surface. The first layer height is taken as 10^{-5} m for the desired $y+$ as 20.

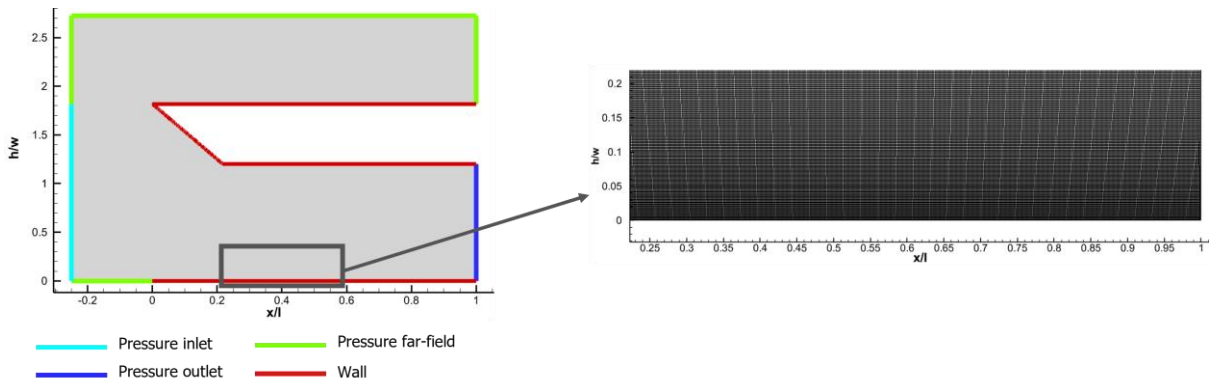

Fig 4. Computation grid for $h/w = 1.82$ configuration.

3.3. Grid independence and methods validation.

The grid independence study was investigated for the oblique shock impingement on the flat plate in inviscid flow condition for $h/w = 1.82$. The mesh density was varied by systematically changing the global element size. The coarsest mesh had 45908 elements, while the finest mesh had 342960 elements. A medium mesh with 216292 elements is a compromise between the detailed resolution of the fine mesh and the efficiency of the coarse mesh offering a balance between accuracy and computational time and is therefore chosen for all simulations conducted in this study to assess the grid independence, the variation of normalised wall pressure on flat plate is shown in the Fig. 5.

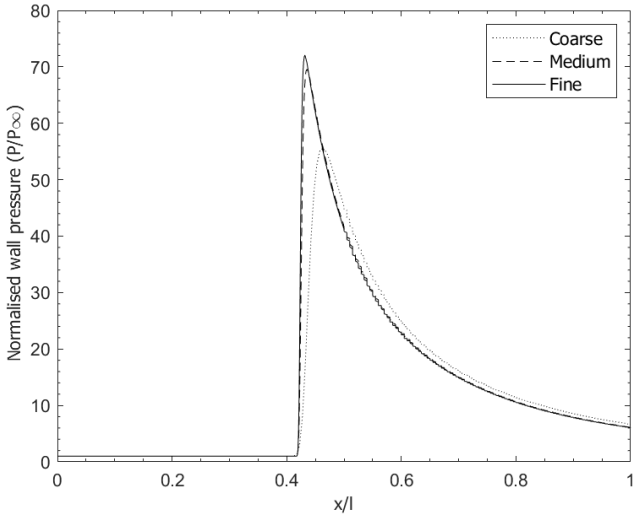

Fig 5. Grid Independence study for the case: $h/w = 1.82$.

For validating the numerical method, the computational data are compared with the experimental data as shown in Fig. 6 to assess the predicted normalized wall pressure variation [1]. The experimental model using shock generator 12° creates an impinging shock on a flat plate at flow conditions of Mach 7 (2.44 MJ kg^{-1}) with free stream unit Reynolds number of 4.93 x 10^6 m^{-1}. A numerical investigation was conducted using the ANSYS Fluent software to simulate the phenomenon under study. A two-dimensional, density-based formulation was employed for both laminar and detached eddy simulation (DES) turbulence model. A comprehensive numerical method study has assessed the suitability of the chosen method. The results demonstrated good agreement between the predicted separation and reattachment points and published experimental data, indicating that the chosen method is well-suited for capturing the essential flow physics of the investigated phenomenon. It is important to acknowledge that inherent numerical errors resulted in slight deviations between the predicted peak pressure and the experimental measurements. Nevertheless, the simulations successfully captured the desired flow characteristics at the designated wall locations.

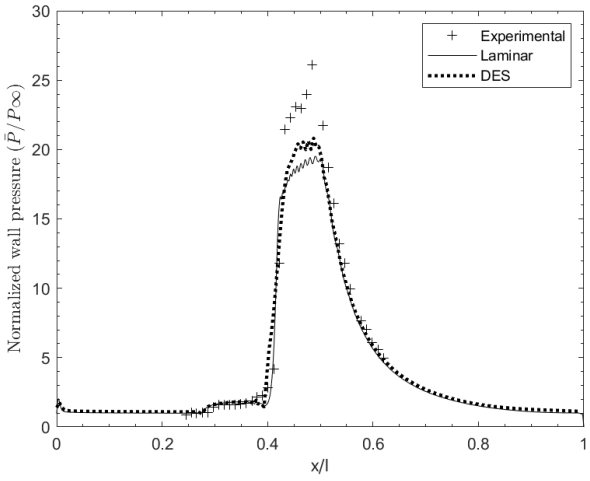

Fig 6. Method validation for DES and Laminar flow solver

4. Results and Discussion

The numerical studies on the interaction of oblique shock from wedge on a flat plate illustrated in the Fig. 3 is carried out for h/w ratios of 1.82 and 1.73. The influence of h/w ratio for the oblique shock on flat plate is studied in inviscid flow condition and consequently assessed for boundary layer in the flow field. The results are categorized into the following subsections, addressing:

4.1. The variation of h/w ratio for inviscid flow condition.

The present study investigates the influence of wedge position vertically above the flat plate (h/w). The wedge is positioned in a streamwise direction, aligning its leading edge with the flat plate. By varying h/w, the oblique shock impingement location is systematically modified. Due to the inviscid nature of the analysis, the impingement locations obtained are considered as exact solutions.

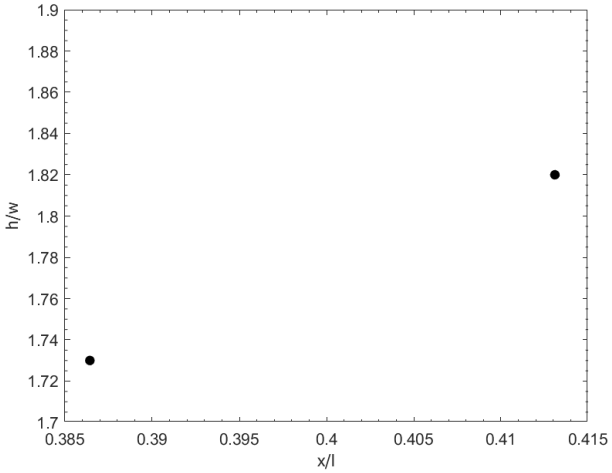

Fig 7. Variation of oblique shock impingement location on flat plate for $h/w = 1.82 \,\&\, 1.73$ in inviscid flow at Mach 6.

Fig. 7 illustrates the variation of oblique shock impingement locations along the flat plate as function of h/w. These observations reveal a critical relationship: as the wedge is gradually moved away from the flat plate (increasing h/w), the shock impingement location correspondingly shifts downstream. Conversely, bringing the wedge closer to the flat plate (decreasing h/w) results in an upstream shift of the impingement point. It is noteworthy that the location of shock impingement exhibits an upstream movement of 5.33 mm for h/w from 1.82 to 1.73. This finding holds significant implications for achieving precise control over shock wave reflection on flat plates. It signifies that the desired reflection characteristics can be attained by strategically positioning the shock impingement location by carefully manipulating the wedge position, specifically the h/w ratio.

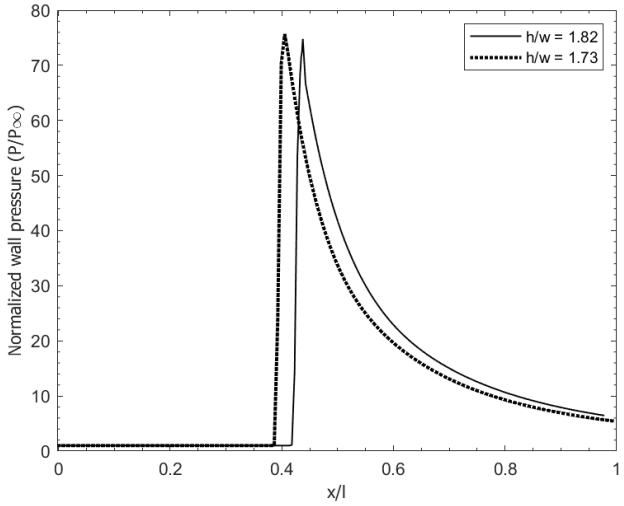

Fig 8. Normalized wall pressure ratio on flat plate in inviscid Mach 6 flow for $h/w = 1.82 \,\&\, 1.73$.

Fig. 8 presents the normalized wall pressure distribution on flat plate for varying h/w ratios. The peak normalized pressure obtained in the figure denotes the impinging oblique shock strength on the flat plate. Interestingly, the peak normalized pressure ratio decreases by $1.174\,\%$ as h/w increases from 1.73 to 1.82. This decrease in peak pressure attributes to decreased shock strength of the impinging oblique shock. This observed phenomenon can be attributed primarily to the influence of the Prandtl-Meyer expansion (PME) emanating from the wedge corner wherein a comparatively more spatial domain is available between the PME and the impinging oblique shock wave for interaction and leads to a

progressive weakening of the oblique shock strength with increase in h/w. However, the significant weaking of the impinging oblique shock strength can be observed for larger values of h/w and requires further investigation. The Fig. 9 denotes Mach isoline contour for h/w ratios of 1.82 and 1.73. The reflection observed in these cases is a regular reflection (RR). The upstream movement of oblique shock impingement location can be observed. The interaction zone between the impinging oblique shock and PME is highlighted in the figure below.

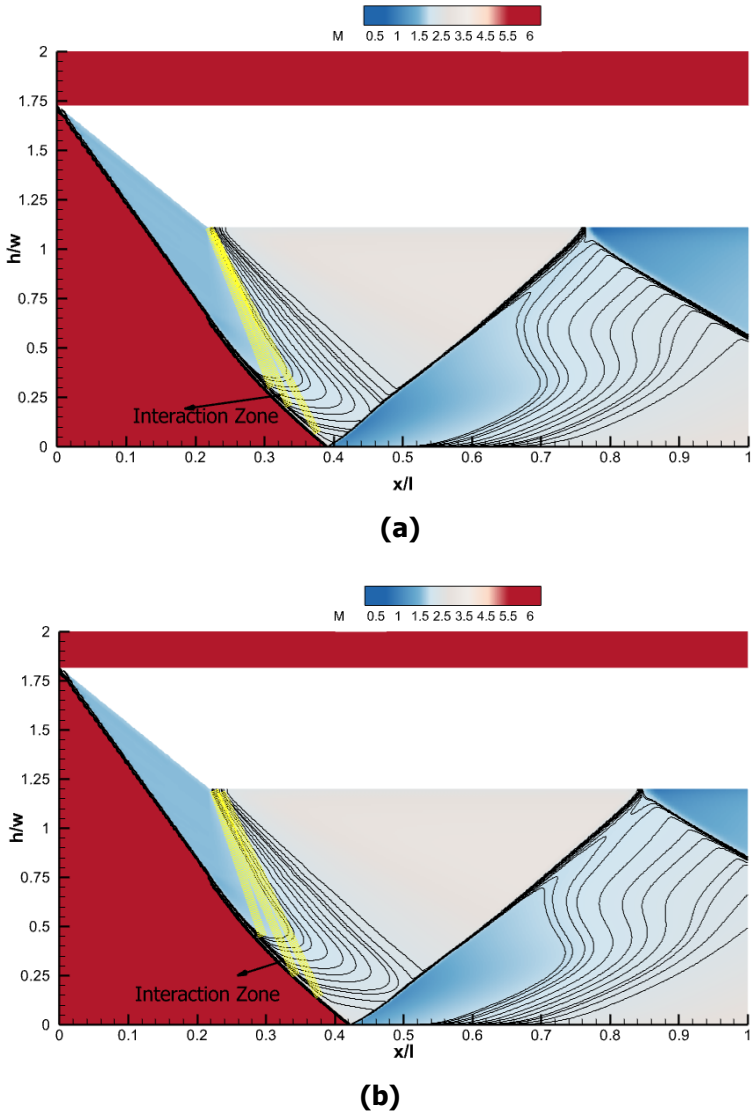

Fig 9. Mach isoline contour at Mach 6 in steady inviscid flow for various h/w ratios (a) h/w = 1.73 (b) h/w = 1.82. The obtained reflection for the above cases is RR and upstream movement of oblique shock impingement location and interaction zone can be observed.

4.2. The variation of h/w and its influence on boundary layer for oblique shock impingement.

The current study investigates the influence of h/w for 1.82 & 1.73 on the boundary layer of flat plate at the constant streamwise position of the wedge. The presence of the boundary layer for the impinging oblique shock creates adverse pressure gradient and consequently separates flow on the flat plate, creating a complex shock structure in the flow field. This shock structure reveals various distinguished flow features in the schlieren image frame for h/w = 1.82 in Fig.10. This interaction between the impinging oblique shock, the leading edge (LE) shock, the near normal shock, the reflected shock and the transmitted shock forms an Edney Type II interaction. This interaction is characterized by the formation of a distinct Mach stem between the two triple points: one formed by the impinging shock,

reflected shock, and Mach stem (TP_1); and another by the LE shock, transmitted shock, and Mach stem (TP_2). The separation length is defined as the distance between the separation shock and the reattachment shock with a subsonic recirculating bubble known as separation bubble. The LE shock angle (β_{LS}) and separation angle (β_{SS}) are formed by the LE shock and separation shock respectively. The presence of a near normal shock in this type of shock interaction within high-speed intakes leads to degradation due to stagnation pressure loss.

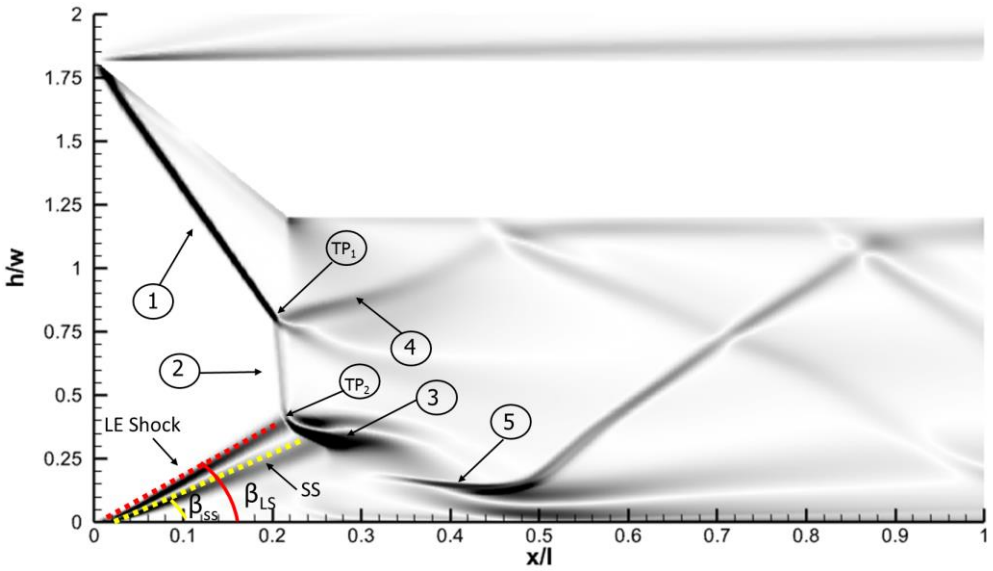

Fig 10. Representation of schlieren image frame for flow features at Mach 6 impinging oblique shock interaction with boundary layer for $h/w = 1.82$ (1) Impinging oblique shock (2) Mach stem (3) Transmitted shock (4) Reflected Shock (5) Reattachment shock. Two distinct triple points (TP_1 & TP_2), and the LE shock and separation shock (SS), and its angles are also denoted.

In the context of strong SWBL interactions, the impinging oblique shock can manifest as either a regular reflection or a Mach reflection. At h/w of 1.82 & 1.73, the interaction primarily results in RR for inviscid flow conditions as observed in the Fig. 9, however, with influence of boundary layer on the flat plate this interaction transforms into Mach reflection. The separated flow creates an upstream influence in the boundary layer forming a separation bubble consequently resulting in separation shock due to incoming hypersonic flow. The subsonic channel downstream of the near normal shock in this flow structure is accelerated until sonic throat appears after which the flow turns into supersonic. This is well illustrated in Fig. 11(a) and 12(a) which presents time-averaged Mach isoline contour for $h/w = 1.82$ & 1.73, capturing the influence of impinging shock boundary layer interaction across the flow field. Notably, the interaction of impinging oblique shock from the wedge, LE shock from the flat plate and near normal shock formed in the flow field can easily be observed in the two cases from the Fig 11(b) and 12(b) depicting schlieren image frame. With decrease of h/w from 1.82 to 1.73, the triple point (TP_2) formation from the former shocks shows an upstream movement by 6.83 mm and an increase in Mach stem height of 4.16 mm in the flow field.

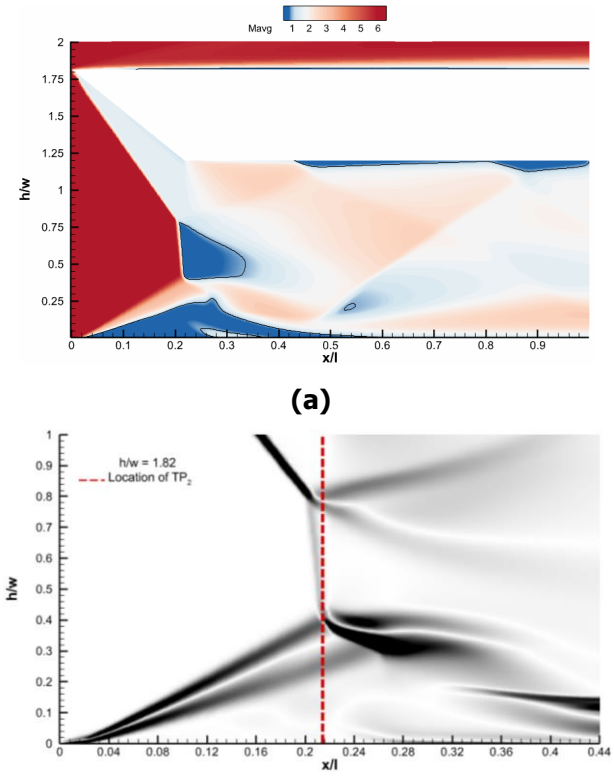

Fig 11. (a) Time-averaged Mach flow contour depicting Mach isoline for h/w = 1.82 at Mach 6. (b) Schlieren image for close up view of Edney Type II interaction for h/w = 1.82 at Mach 6

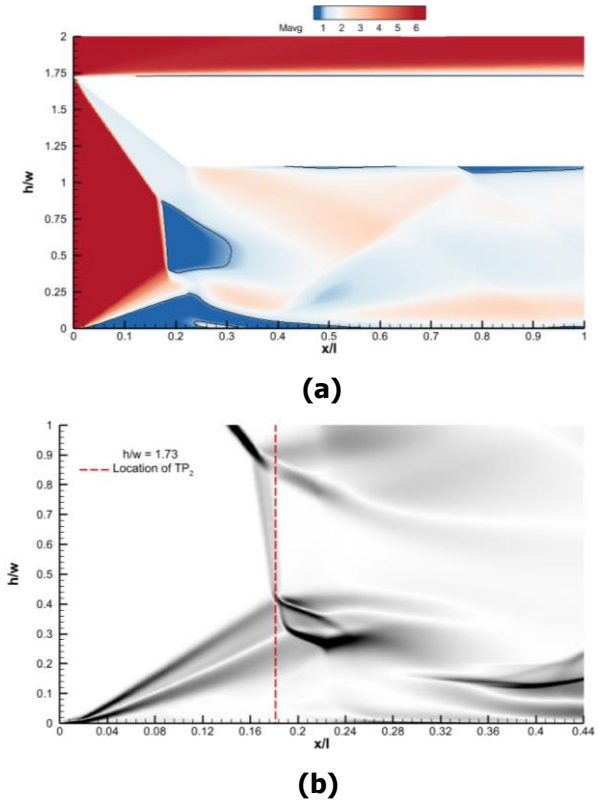

Fig 12. (a) Time-averaged Mach flow contour depicting Mach isoline for h/w = 1.73 at Mach 6. (b) Schlieren image for close up view of Edney Type II interaction for h/w = 1.73 at Mach 6

The influence of h/w ratio on time-averaged normalized wall pressure on the flat plate is illustrated in the Fig. 13. The vertical line indicates the inviscid shock impingement location for the respective h/w ratio. The study reveals that the initial rise in the normalized pressure denotes the presence of LE shock, and the strength of the LE shock remains constant for h/w ratio 1.82 & 1.73. The plateau pressure observed denotes the separation bubble length in the flow field. The magnified view of the plateau pressure for h/w ratio of 1.82 & 1.73 is denoted Fig. 14. From the figure, a rise in plateau pressure and fall of separation bubble length can be identified for decrease in h/w ratio from 1.82 to 1.73.

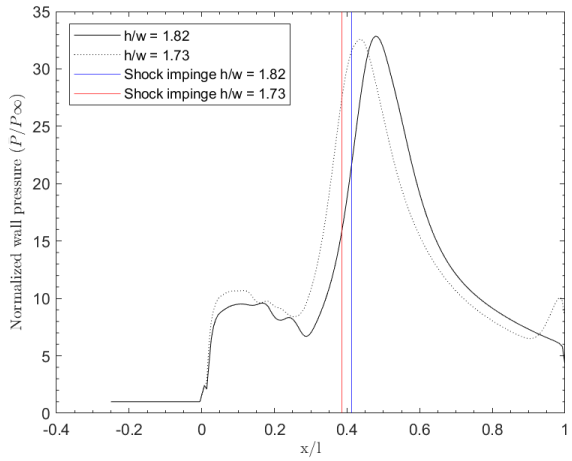

Fig 13. Time-averaged normalized wall pressure distribution on flat plate for h/w ratios for 1.82 & 1.73 in Mach 6 flow condition.

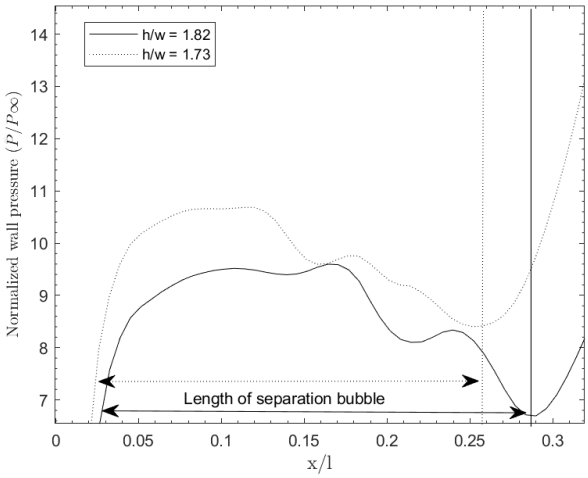

Fig 14. Magnified view of the plateau pressure indicating separation shock and length of separation bubble for h/w = 1.82 and 1.73 at Mach 6 flow conditions.

Table 2. Influence of h/w on flow characteristics at Mach 6 flow conditions

Vertical distance ratio	h/w = 1.82	h/w = 1.73
$\boldsymbol{\beta_{LS}}$	30°± 6.5%	32°± 6.5%
$\boldsymbol{\beta_{SS}}$	15° ± 6.5%	16° ± 6.5%
Separation bubble length	51.46 mm	46.41 mm
Mach stem height	20 mm	24.16 mm
Triple point (TP_2) location (x/l)	0.215	0.182

Table 2 presents influence of h/w on flow characteristics for MR in presence of boundary layer on a flat plate. The data suggests minimal variations in the LE and separation shock angles associated with the LE and separation shock. However, a significant decrease of 9.8% in the separation bubble length is evident with decrease in h/w . Conversely, the Mach stem height demonstrates a notable increase by 20%. These variations are accompanied due to the phenomenon of an upstream migration of the oblique shock impingement location with decreasing h/w. As the shock impinges downstream of the boundary layer, it creates a longer separated flow resulting in longer recirculation bubble length and consequently the interaction of the shocks (LE, transmitted and near normal shock) takes place downstream. With decreasing of h/w, the separated flow making an upstream influence is smaller in length and results in the interaction of the shocks to take place comparatively upstream of the flow. Hence, for the longer separation bubble, the reattachment shock location (peak normalized pressure in Fig.13) is comparatively downstream for $h/w = 1.82$ & 1.73. Hence, the triple point (TP_2) location is higher for $h/w = 1.82$ case as compared to $h/w = 1.73$ indicating the movement of interaction of shocks. Therefore, in conclusion, by increasing h/w from 1.73 to 1.82, downstream impingement of oblique shock from the wedge is obtained consequently creating a longer separation bubble length, lower Mach stem height and interaction of shocks moving downstream.

5. Conclusions and future work.

The successful realization of influence of h/w on flow characteristics for MR over a flat plate is observed in this study. This study reveals a noteworthy observation: at higher freestream Mach number and wedge angle approaching the flow detachment angle, regular reflections in the inviscid flow turn to Mach reflection in the presence of boundary layer. The effect of movement of oblique shock impingement location along flat plate on separation bubble length and Mach stem height is studied. Future investigations should focus on the unsteadiness of the separation bubble and the modal behaviour of the near-normal shock. To better understand this flow physics, subsequent experimental research will be conducted in the S1 Hypersonic facility at HEAL.

6. Acknowledgements

The authors gratefully acknowledge the Hypersonic Experimental Aerodynamics Laboratory (HEAL) for providing access to the facilities utilized in this research. The invaluable access to the High-Performance Computing (HPC) facility at the Indian Institute of Technology Kanpur is acknowledged for facilitating research developments.

References.

1. Chang, E., Chan, W., McIntyre, T., & Veeraragavan, A. (2022). Hypersonic shock impingement studies on a flat plate: Flow separation of laminar boundary layers. Journal of Fluid Mechanics, 951, A19. doi:10.1017/jfm.2022.827
2. Sun, Z., Tian, G., & Wu, Y. (2020). Shock-Wave/Boundary-Layer interactions at compression ramps studied by High-Speed Schlieren. AIAA Journal, 58(4), 1681–1688. doi:10.2514/1.j058257
3. Papamoschou, D., & Johnson, A. (2006). Unsteady phenomena in supersonic nozzle flow separation. 36th AIAA Fluid Dynamics Conference and Exhibit. doi:10.2514/6.2006-3360
4. Murugan, J. N., & Govardhan, R. N. (2020). Study of shock wave-boundary layer interaction using high-speed schlieren imaging. Journal of Flow Visualization and Image Processing, 27(2), 185– 97. doi:10.1615/jflowvisimageproc.2020031044
5. Délery J. Physical Introduction. In: Babinsky H, Harvey JK, eds. Shock Wave-Boundary-Layer Interactions. Cambridge Aerospace Series. Cambridge University Press; 2011:5-86.
6. Hornung, H. G. (1986). Regular and Mach reflection of shock waves. Annual Review of Fluid Mechanics, 18(1), 33–58. doi:10.1146/annurev.fl.18.010186.000341
7. Grossman, I. J., & Bruce, P. J. (2018). Confinement effects on regular–irregular transition in shock-wave–boundary-layer interactions. Journal of Fluid Mechanics, 853, 171–204. doi:10.1017/jfm.2018.537

8. Matheis, J., & Hickel, S. (2015). On the transition between regular and irregular shock patterns of shock-wave/boundary-layer interactions. Journal of Fluid Mechanics, 776, 200–234. doi:10.1017/jfm.2015.319
9. Edney, B. E. (1968). Anomalous heat transfer and pressure distributions on blunt bodies at hypersonic speeds in the presence of an impinging shock. doi:10.2172/4480948
10. Meerts, C., Steelant, J., & Hendrick, P. (2011). Preliminary design of the low speed propulsion air intake of the LAPCAT-MR2 aircraft. ESASP, 692, 38. http://ui.adsabs.harvard.edu/abs/2011ESASP.692E..38M/abstract
11. Liepmann, H. W., Roshko, A., & Dhawan, S. (1952, January 1). On Reflection of Shock Waves from Boundary Layers. NASA Technical Reports Server (NTRS). https://ntrs.nasa.gov/citations/19930090967
12. Degrez, G., Boccadoro, C., & Wendt, J. (1987). The interaction of an oblique shock wave with a laminar boundary layer revisited. An experimental and numerical study. Journal of Fluid Mechanics, 177, 247-263. doi:10.1017/S0022112087000946
13. Yao, Y., Li, S., & Wu, Z. (2013). Shock reflection in the presence of an upstream expansion wave and a downstream shock wave. Journal of Fluid Mechanics, 735, 61-90. doi:10.1017/jfm.2013.467
14. Childs, M. E., Hijman, R., & Miller, D. S. (1964). Mach 8 to 22 studies of flow separations due to deflected control surfaces. AIAA Journal, 2(2), 312–321. https://doi.org/10.2514/3.2289
15. Needham, D., & Stollery, J. L. (1966). Boundary layer separation in hypersonic flow. 3rd And 4th Aerospace Sciences Meeting. https://doi.org/10.2514/6.1966-455
16. Sriram, R., Srinath, L. S., Devaraj, M. K. K., & Jagadeesh, G. (2016). On the length scales of hypersonic shock-induced large separation bubbles near leading edges. Journal of Fluid Mechanics, 806, 304–355. https://doi.org/10.1017/jfm.2016.591
17. Paramanantham, V., Janakiram, S., & Rajesh, G. (2022). Prediction of Mach stem height in compressible open jets. Part 1. Overexpanded jets. Journal of Fluid Mechanics, 942. https://doi.org/10.1017/jfm.2022.374
18. Hornung, H. G., & Robinson, M. (1982). Transition from regular to Mach reflection of shock waves Part 2. The steady-flow criterion. Journal of Fluid Mechanics, 123, 155–164. https://doi.org/10.1017/s0022112082003000
19. Иванов, М. С., Vandromme, D., Fomin, V. M., Kudryavtsev, A. N., Hadjadj, A., & Khotyanovsky, D. V. (2001). Transition between regular and Mach reflection of shock waves: new numerical and experimental results. Shock Waves, 11(3), 199–207. https://doi.org/10.1007/pl00004075
20. Schmisseur, J.D., Gaitonde, D.V. Numerical simulation of Mach reflection in steady flows. Shock Waves 21, 499–509 (2011). https://doi.org/10.1007/s00193-011-0335-x
21. Chen, Z., Bai, C., & Wu, Z. (2020). Mach reflection in steady supersonic flow considering wedge boundary-layer correction. Chinese Journal of Aeronautics, 33(2), 465–475. https://doi.org/10.1016/j.cja.2019.09.007
22. Matheis, J., & Hickel, S. (2015). On the transition between regular and irregular shock patterns of shock-wave/boundary-layer interactions. Journal of Fluid Mechanics, 776, 200–234. https://doi.org/10.1017/jfm.2015.319
23. Ansys fluent 12.0 theory guide - 4.10.3 SST k-w Based DES Model
24. Ansys fluent 12.0 theory guide - 9.5 Inviscid Flows